International Tables for Crystallography (2018). Vol. H, Figure 2.8.8, p. 180.

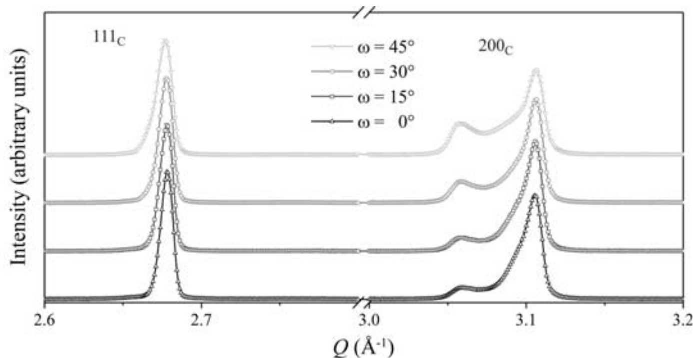

Figure 2.8.6
111_C and 200_C reflections of bipolar fatigued PIC 151 (50 Hz, 10^7 cycles) in the remanent state (0 kV mm^{-1} at $\omega = 0°$, 15°, 30° and 45°).

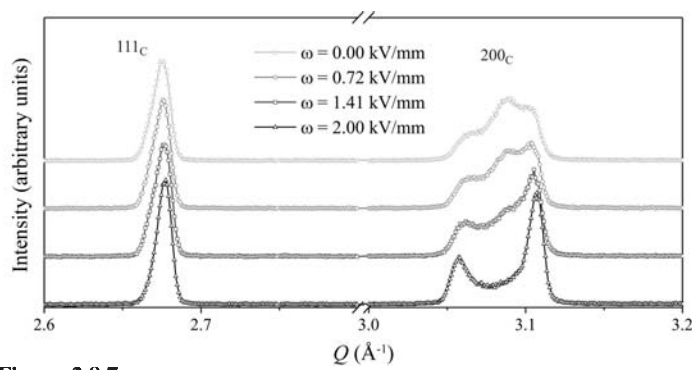

Figure 2.8.7
111_C and 200_C reflections of bipolar fatigued PIC 151 (50 Hz, 10^7 cycles) at $\omega = 45°$ with 0.0, 0.72, 1.41 and 2.0 kV mm^{-1}.

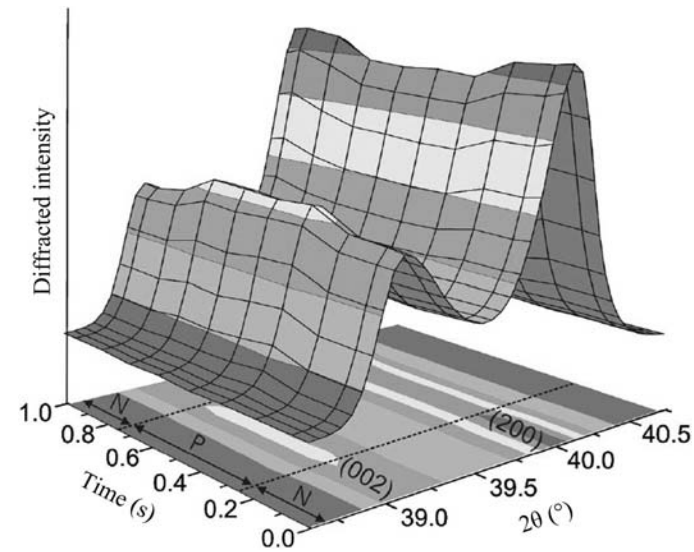

Figure 2.8.8
Diffracted intensities of the pseudo-cubic 002 reflections as a function of 2θ and time during application of a square, bipolar electric field waveform of frequency 1 Hz and amplitude of plus or minus half the coercive field. The timescale is described using eight steps. The positive (P) state of the electric field is applied between 0.25 and 0.75 s, which is bounded on either side by the negative (N) field state. The diffraction vectors 002 and 200 are parallel to the applied electric field. Reproduced with permission from Jones *et al.* (2006). Copyright (2006) AIP Publishing.

resolution of 1 ms only one intermediate step is observed (Fig. 2.8.9*a*). With a time resolution of 250 µs a significant number of intermediate steps can be studied (Fig. 2.8.9*b*). The commercially available soft-doped PZT material EC-65 has also been observed under the application of an electric field and mechanical stress. Lattice strains were measured under cyclic electric fields at times as short as 30 µs (Pramanick *et al.*, 2010).

The use of lead-containing materials may in the future be banned because of environmental concerns, hence considerable efforts are being made to find materials with properties similar to PZT. Only a few elements (Ba, Bi, Na, K, Nb, Ti) seem to be suitable. Nevertheless, a combination of the relevant oxides of these leads to a large variety of potential materials. $(Bi_{0.5}Na_{0.5})TiO_3$–$BaTiO_3$ (BNT–BT) (Hinterstein, Schmitt *et al.*, 2015), $(Bi_{0.5}Na_{0.5})TiO_3$–$(Bi_{0.5}K_{0.5})TiO_3$ (BNT–BKT) (Levin *et al.*, 2013), BNT–BT–$K_{0.5}Na_{0.5}NbO_3$ (BNT–BT–KNN) (Schmitt *et al.*, 2010), BNT–BKT–KNN (Anton *et al.*, 2012) and BNT–KNN (Liu *et al.*, 2017) are the focus of most attention. The materials in the $(1 - x - y)$BNT–xBT–yKNN system exhibit remarkable piezoelectric properties over a narrow composition range $0.05 \leq x \leq 0.07$ and $0.01 \leq y \leq 0.03$ (Zhang *et al.*, 2007). Daniels *et al.* (2010) proposed a combinatorial approach to studying a range of compositions in a single sample, where different stoichiometries created a compositional gradient in the sample. A limited number of bulk homogeneous samples were prepared for comparison. Microfocus X-ray beams from a synchrotron allowed investigation of the gradient material under a field.

Fig. 2.8.10 displays the diffraction patterns under an external electric field up to 5.5 kV mm^{-1}. Data analysis was performed by fitting the data of the pseudo-cubic 002 reflection to distorted pseudo-cubic and tetragonal symmetry for each composition and electric field. Whereas in the 0.86BNT–0.14KNN composition only a distorted pseudo-cubic behaviour is observed

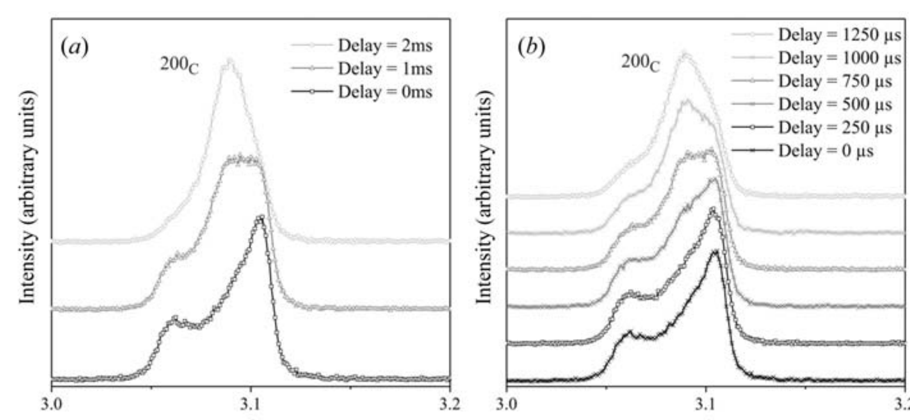

Figure 2.8.9
Pump–probe measurements of the 200_C reflection at $\omega = 45°$. Cycling switching between the remanent and the applied field state at 2 kV mm^{-1} with 50 Hz and a time resolution of (*a*) 1 ms and (*b*) 250 µs. Only a time resolution of 250 µs results in sufficient intermediate steps between the remanent and the poled state to study the processes during poling.